


Trapping and Ground-State Cooling of a Single H_2^+

N. Schwegler¹,* D. Holzapfel¹, M. Stadler¹, A. Mitjans¹, I. Sergachev¹, J. P. Home¹, and D. Kienzler¹
*Institute for Quantum Electronics, Department of Physics, Eidgenössische Technische Hochschule Zürich,
 Otto-Stern-Weg 1, 8093 Zurich, Switzerland*

 (Received 14 December 2022; revised 24 April 2023; accepted 24 July 2023; published 27 September 2023)

We demonstrate co-trapping and sideband cooling of a $\text{H}_2^+ - {}^9\text{Be}^+$ ion pair in a cryogenic Paul trap. We study the chemical lifetime of H_2^+ and its dependence on the apparatus temperature, achieving lifetimes of up to 11_{-3}^{+6} h at 10 K. We demonstrate cooling of two of the modes of translational motion to an average phonon number of 0.07(1) and 0.05(1), corresponding to a temperature of 22(1) and 55(3) μK , respectively. Our results provide a basis for quantum logic spectroscopy experiments of H_2^+ , as well as other light ions such as HD^+ , H_3^+ , and He^+ .

DOI: [10.1103/PhysRevLett.131.133003](https://doi.org/10.1103/PhysRevLett.131.133003)

The hydrogen molecular ion is the simplest stable molecule and its internal structure can be calculated to very high precision, making it a valuable platform for determining fundamental constants and testing theory [1,2]. However, H_2^+ is difficult to study experimentally: its bound electronic excited states have negligible transition probabilities to low rovibrational states of the electronic ground state and, due to its nonpolar nature, rovibrational transitions are dipole forbidden resulting in extremely long lifetimes for most excited rovibrational states (weeks and longer) [3,4]. These properties make direct laser cooling, internal readout by state-dependent fluorescence detection, and state preparation by optical pumping impossible. Additionally, it readily reacts with H_2 , which is the primary background gas in ultrahigh vacuum (UHV) systems, limiting trapping lifetimes.

Only few contemporary H_2^+ high-precision spectroscopy experiments exist, reflecting these experimental challenges. The LKB Paris experiment uses a Paul trap to confine ≈ 100 H_2^+ ions together with co-trapped ${}^9\text{Be}^+$ ions for sympathetic cooling with the goal of interrogating the fundamental vibrational transition. Rovibrational state preparation is performed by resonance-enhanced multiphoton ionization (REMPI) of H_2^+ and readout by state-dependent photodissociation [5]. Trapping lifetimes of the H_2^+ ions are limited by chemical reactions to a few minutes and their temperature is $\mathcal{O}(10)$ mK [6]. Similar techniques have enabled high-precision spectroscopy of the heteronuclear isotopologue HD^+ and in combination with theory provided a determination of the proton-to-electron mass ratio to a relative uncertainty of 2×10^{-11} [7,8].

The ETH Zürich Molecular Physics and Spectroscopy group utilizes Rydberg spectroscopy of a neutral H_2 beam to extract properties of H_2^+ via multichannel quantum-defect theory [9,10]. This has enabled a measurement of the ortho- H_2^+ hyperfine structure [11] and a determination of

the first rotational interval of para- H_2^+ with relative frequency uncertainty of 4.4×10^{-7} [12].

High-precision mass measurements have been performed using hydrogen molecular ions confined in Penning traps [13–17]. In these experiments, the ions have been cooled to ≈ 1 K by coupling to cryogenic electrical circuits and trapping lifetimes in excess of several months have been observed [17].

Optical spectroscopy of hydrogen molecular ions is expected to profit from experiments using trapped single H_2^+ ions due to the suppression of systematic uncertainties. Selected rovibrational transitions in H_2^+ are projected to reach a relative frequency uncertainty of $\mathcal{O}(10^{-17})$ [1,18]. First steps towards high-precision spectroscopy of single hydrogen molecular ions have been demonstrated recently using co-trapped $\text{HD}^+ - {}^9\text{Be}^+$ pairs [19]. However single-ion experiments suffer from low signal and to be performed efficiently necessitate state preparation and a high spectroscopy duty cycle, i.e., reducing the duration or frequency of overhead operations like ion loading and state preparation. For H_2^+ this challenge is amplified by several issues: It is created by ionizing H_2 , which requires some H_2 density, but also reacts strongly with H_2 to H_3^+ , limiting trapping lifetimes in case the ionization is performed in the trapping volume. Rovibrational state preparation will likely increase this challenge: Buffer-gas cooling with He was proposed, but is slow and will thus likely require long H_2^+ lifetimes [20]. Preparation of the H_2^+ rovibrational state using REMPI typically requires a H_2 beam intersecting with the trapping volume, further increasing the H_2 concentration and thus lowering the H_2^+ lifetime [5]. These issues can be overcome by increased H_2 pumping speed and long trapping lifetimes.

Quantum logic spectroscopy (QLS) has been shown to allow pure quantum-state preparation and quantum non-demolition readout even for hard to control ion species.

In this technique a second, well-controlled ion species is co-trapped to exert control over the ion of interest through quantum gate operations which couple both ions to a shared normal mode of motion [21]. QLS has been used in the most accurate atomic clock and for quantum control and spectroscopy of highly-charged ions and molecular ions [22–28]. It is a frequently suggested method to improve spectroscopy of H_2^+ but has not been implemented thus far [1,20,25,29,30].

In this Letter we demonstrate trapping of single $\text{H}_2^+ - {}^9\text{Be}^+$ ion pairs with a lifetime of 11_{-3}^{+6} h and ground-state cooling of two of the normal modes of the ion pair’s translational motion to a temperature of 22(1) and 55(3) μK , respectively. Our achieved H_2^+ lifetime should enable us to utilize buffer-gas cooling for rovibrational ground-state preparation and in combination with QLS to prepare pure quantum states of H_2^+ as a starting point for high-precision spectroscopy [20]. Ground-state cooling is a first step in many implementations of QLS and can be used to reduce the second-order Doppler shift caused by the ions’ secular motion [21,31–34].

The ions are trapped in a monolithic, microfabricated linear Paul trap housed in a UHV chamber with an inner chamber cooled by a liquid helium flow cryostat. Single beryllium ions are loaded in the trap volume by photo-ionization of neutral beryllium atoms emitted from a thermal oven, while H_2^+ is loaded through electron-impact ionization of residual gas molecules. The choice of ${}^9\text{Be}^+$ as cooling ion is due to it being the lightest well-controlled ion species, providing sufficient participation of the two ions in shared normal modes of motion [35].

Experiments primarily operate using the following sequence: Doppler cooling of ${}^9\text{Be}^+$ and initialization of ion order, ${}^9\text{Be}^+$ spin-state preparation by optical pumping, experiment-specific pulses, and finally ${}^9\text{Be}^+$ hyperfine state readout using state-dependent fluorescence captured by a photomultiplier tube [36]. Most operations on ${}^9\text{Be}^+$ use 313 nm laser light to couple the ${}^9\text{Be}^+$ electronic ground state $S_{1/2}$ to the excited P manifold. We use microwaves to drive magnetic dipole transitions in the ${}^9\text{Be}^+$ $S_{1/2}$ hyperfine manifold.

We implement loading of $\text{H}_2^+ - {}^9\text{Be}^+$ by first trapping a single ${}^9\text{Be}^+$ ion, which we detect by imaging its fluorescence light onto a CMOS camera. By performing real-time image analysis, we continuously monitor its axial position. To load an H_2^+ ion we use an electron beam that ionizes the residual gas in the vacuum chamber. When an ion is loaded, it is sympathetically cooled by the ${}^9\text{Be}^+$ ion in the trap. We cannot observe this “dark ion” directly as it does not fluoresce, but since sympathetic cooling causes the ion to crystallise, we detect a shift in the ${}^9\text{Be}^+$ position on the camera image. Since electron bombardment is not species selective we observe loading of several species: We dominantly load He^+ , but also observe loading of ions

heavier than ${}^9\text{Be}^+$, compatible with a mass range of $\approx 14\text{--}20$ u (assuming singly charged cations). We mass selectively remove parasitic ion species by excitation of their motional modes.

More details on the apparatus, control of $\text{H}_2^+ - {}^9\text{Be}^+$, and the loading procedure can be found in the Supplemental Material [37], which includes Refs. [38–41].

To identify the presence of H_2^+ , we perform motional sideband spectroscopy on the ${}^9\text{Be}^+$ spin using a pair of Raman beams. We probe the blue motional sideband spectrum and, in case H_2^+ was loaded, can identify the expected resonances of the axial in- and out-of-phase modes of $\text{H}_2^+ - {}^9\text{Be}^+$. We observe drifts in the sideband resonances of up to $\approx 2\pi \times 10$ Hz s^{-1} , which are likely caused by changing electrical stray fields originating from surfaces charged during the loading procedure. Comparing the in- and out-of-phase resonance frequencies to normal mode calculations enables us to determine both charge and mass of the second trapped ion without precise knowledge of the strength of the trapping potential. The calculations only assume trapping of a single ${}^9\text{Be}^+$ ion and a second ion of variable charge and mass. Using this method, we can distinguish trapping of H_2^+ , H_3^+ , and He^+ , and also exclude potential trapping of, e.g., He^{2+} . Example sideband spectra for ${}^9\text{Be}^+$, $\text{H}_2^+ - {}^9\text{Be}^+$, and $\text{H}_3^+ - {}^9\text{Be}^+$ are shown in Fig. 1.

Because of the limited H_2 pumping speed in UHV chambers, the reaction $\text{H}_2^+ + \text{H}_2 \rightarrow \text{H}_3^+ + \text{H}$ is usually the dominant loss mechanism for H_2^+ and limits the trapping lifetime at typical UHV pressures to a few minutes [6]. The cooled inner chamber allows us to reduce the H_2 partial pressure by cryogenic pumping, extending H_2^+ trapping lifetimes.

To investigate the lifetime of H_2^+ in our apparatus, we load an $\text{H}_2^+ - {}^9\text{Be}^+$ pair and continuously perform measurements to identify the trapped ions. We observe three loss mechanisms: Chemical reaction $\text{H}_2^+ + \text{H}_2 \rightarrow \text{H}_3^+ + \text{H}$, loss of H_2^+ , and loss of ${}^9\text{Be}^+$. To distinguish these cases, we use the ${}^9\text{Be}^+$ fluorescence signal to confirm the presence of ${}^9\text{Be}^+$ and again perform motional sideband spectroscopy on ${}^9\text{Be}^+$ to discriminate single ${}^9\text{Be}^+$, $\text{H}_2^+ - {}^9\text{Be}^+$, and $\text{H}_3^+ - {}^9\text{Be}^+$. Since all signals rely on ${}^9\text{Be}^+$, we cannot measure if H_2^+ is still trapped after ${}^9\text{Be}^+$ was lost. We define the trapping duration of the $\text{H}_2^+ - {}^9\text{Be}^+$ pair as the time difference between the first and last scan showing the signature of $\text{H}_2^+ - {}^9\text{Be}^+$.

We repeat the ion-loss measurement several times and calculate the survival probability $P_{\text{Surv}}(t)$ of the $\text{H}_2^+ - {}^9\text{Be}^+$ pair after a trapping duration of t as $P_{\text{Surv}}(t) = N(t)/N_{\text{tot}}$, where $N(t)$ is the number of ion-loss measurements with trapping duration larger or equal to t and N_{tot} is the total number of ion-loss measurements. We took four data sets at cryostat temperatures of 10, 17, 19, and 22 K, which are shown in Fig. 2. Estimations of the thermal conductance and heat load in our apparatus suggest that the

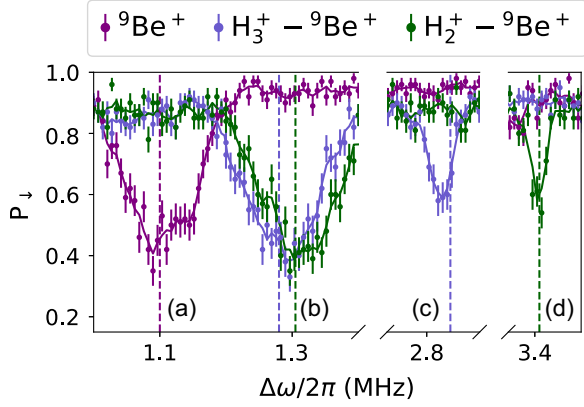


FIG. 1. Example of sideband spectroscopy scans on ${}^9\text{Be}^+$ probing the axial mode frequencies to distinguish $\text{H}_2^+ - {}^9\text{Be}^+$, $\text{H}_3^+ - {}^9\text{Be}^+$, and ${}^9\text{Be}^+$. The detuning of the Raman lasers from the carrier transition is denoted $\Delta\omega$ and the measured ${}^9\text{Be}^+$ $|\downarrow\rangle$ probability P_{\downarrow} . The solid lines represent a running average over three points to guide the eye. The vertical dashed lines mark the calculated frequency of the in- and out-of-phase axial mode of $\text{H}_2^+ - {}^9\text{Be}^+$ and $\text{H}_3^+ - {}^9\text{Be}^+$ based on the axial frequency of a single ${}^9\text{Be}^+$ ($2\pi \times 1.1$ MHz) confined in the same trapping potential. Different frequency ranges use different probe duration to optimize signal strength. The sets for $\text{H}_2^+ - {}^9\text{Be}^+$ and $\text{H}_3^+ - {}^9\text{Be}^+$ are taken a few minutes apart, during which H_2^+ underwent a chemical reaction to H_3^+ . The mass changed from 2 to 3 u, which shifts (b) the axial in-phase mode at $2\pi \times 1.3$ MHz by $-2\pi \times 25$ kHz, and the axial out-of-phase mode is shifted from (d) $2\pi \times 3.4$ to (c) $2\pi \times 2.8$ MHz. A single ${}^9\text{Be}^+$ shows a resonance in scan (a) only, giving us a means of detecting loss of H_2^+ . The duration to complete one set of data containing all four scans is 80 s.

corresponding temperature of the inner chamber housing the trap is < 5 K warmer than the measured cryostat temperature. At lower temperatures we observe the

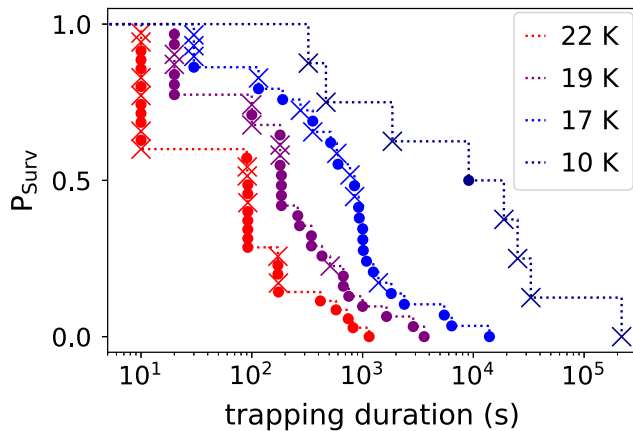


FIG. 2. Survival probability P_{Surv} of $\text{H}_2^+ - {}^9\text{Be}^+$ measured for different cryostat temperatures. For clarity, the data at 22 K (19 K, 17 K) is offset by 10 s (20 s, 30 s). A chemical reaction $\text{H}_2^+ + \text{H}_2 \rightarrow \text{H}_3^+ + \text{H}$ is marked with a circle, while ion loss is marked with a cross. The data is not preprocessed and no additional loss mechanisms are observed.

expected reduced chemical reaction rate, which is consistent with increased cryogenic pumping of the residual H_2 gas. While ion loss is present at all temperatures and also reduces with lower cryostat temperature, it is the dominant loss channel for the 10 K dataset. The entire dataset (all cryostat temperatures combined) contains a total of 103 events, 68 of which are chemical reactions, 24 are loss of H_2^+ and 11 are loss of ${}^9\text{Be}^+$. Of the ${}^9\text{Be}^+$ loss events, seven can be directly correlated with issues of the experiment control system and stability of the ${}^9\text{Be}^+$ cooling laser. The mechanism responsible for H_2^+ loss remains unclear. In separate experiments where we block the ${}^9\text{Be}^+$ cooling laser for a certain duration, we observe H_2^+ loss while ${}^9\text{Be}^+$ stays trapped. The uncooled trapping duration of H_2^+ was a few seconds during the time the dataset was acquired. We have observed an improvement to approximately 10 s since then.

From the survival probability data we derive the $\text{H}_2^+ - {}^9\text{Be}^+$ lifetime, shown in Fig. 3(a). We assume an exponential distribution to simplify the estimation of the error bars, albeit the observed survival probabilities seem to follow a more complex distribution. The lifetime, which includes all loss channels, increases from only a few minutes at 22 K to $\tau = 11_{-3}^{+6}$ h at 10 K. Because we can distinguish ion loss from the $\text{H}_2^+ + \text{H}_2 \rightarrow \text{H}_3^+ + \text{H}$ reaction we can calculate the reaction rate for each cryostat temperature by dividing the total observation time by the number of observed reactions. The reaction rate coefficient is known and well approximated by the Langevin collision rate coefficient $k_L = 2.1 \times 10^{-9} \text{ cm}^3 \text{ s}^{-1}$ [42,43]. This allows us to estimate the partial H_2 density n_{H_2} in the trap volume in dependence of the cryostat temperature, shown in Fig. 3(b). At a cryostat temperature of 10 K we observe a density of $n_{\text{H}_2} = 1.6(1.3) \times 10^3 \text{ cm}^{-3}$. Assuming a temperature of the H_2 gas of 15 K for this density results in an H_2 partial pressure of $p_{\text{H}_2} = 3.3(2.7) \times 10^{-13} \text{ Pa}$.

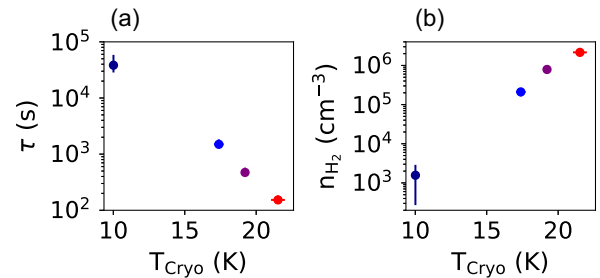


FIG. 3. (a) Lifetime τ of $\text{H}_2^+ - {}^9\text{Be}^+$ and (b) partial H_2 density n_{H_2} for different cryostat temperatures, extracted from the data shown in Fig. 2. The error bars on the y axis show the 68% confidence interval and are derived assuming an exponential distribution. The error bars on the temperature values indicate the standard deviation of the measured temperatures and are limited by the precision of the temperature control loop.

Ground-state cooling of the translational motion of two-ion chains containing a spectroscopy and readout ion is an often-used ingredient for implementing QLS and can also be used to reduce the second-order Doppler shift in spectroscopy caused by the ion's secular motion [21]. Because of the large mass mismatch between H_2^+ and ${}^9\text{Be}^+$, each radial mode has a strong amplitude for only one of the two species, whereas the other ion only participates weakly. In contrast, the two axial modes exhibit a stronger participation of both ions simultaneously, which makes them suitable candidates for the transfer mode in quantum logic protocols [32]. The out-of-phase mode can have advantages for implementing QLS, such as typically reduced heating rates and different mode participation of the ions compared to the in-phase mode. However, in our system, a large ${}^9\text{Be}^+$ Lamb-Dicke parameter of the in-phase mode causes poor contrast on operations on the out-of-phase mode due to the Debye-Waller effect [36]. To achieve high fidelity in QLS operations using the out-of-phase mode, the in-phase mode has to be ground-state cooled as well. We demonstrate ground-state cooling of the axial in-phase mode ($2\pi \times 1.3$ MHz) and axial out-of-phase mode ($2\pi \times 3.4$ MHz) of $\text{H}_2^+ - {}^9\text{Be}^+$ using resolved-sideband cooling on ${}^9\text{Be}^+$ [44]. Because of the high Lamb-Dicke parameter for our Raman beam geometry of $\eta = 0.57$ for the in-phase mode, the thermal state occupation after Doppler cooling is not in the Lamb-Dicke regime and direct cooling to the ground state using the first red sideband only is not possible. Thus, we first use the fourth red sideband to reduce the population to below $n = 4$, followed by sideband cooling using the first red sideband. We implement this in a pulsed fashion, alternating red-sideband pulses with microwave and repumping pulses to reset the spin to $|\downarrow\rangle$. The out-of-phase mode with a Lamb-Dicke parameter of $\eta = 0.1$ can be cooled with only the first red sideband. For simultaneous ground-state preparation of the two axial modes, we first perform ground-state cooling of the in-phase mode as described above, and subsequently ground-state cool the out-of-phase mode. During this step, the in-phase mode gets excited by recoil from the repumping pulses. We therefore follow the out-of-phase cooling with a repetition of the in-phase first-sideband cooling sequence. We estimate the average motional population \bar{n} after both Doppler and ground-state cooling by performing red- and blue-sideband spectroscopy and using the sideband ratio method [36], extracting the sideband contrast through fits to the data and correcting for ${}^9\text{Be}^+$ state-preparation and readout error using data from reference Rabi oscillations driven by microwaves. For the in-phase mode we obtain $\bar{n} = 10(5)$ after Doppler and $\bar{n} = 0.07(1)$ after ground-state cooling. For the out-of-phase mode we obtain $\bar{n} = 2.4(5)$ after Doppler and $\bar{n} = 0.05(1)$ after ground-state cooling. The sideband- and

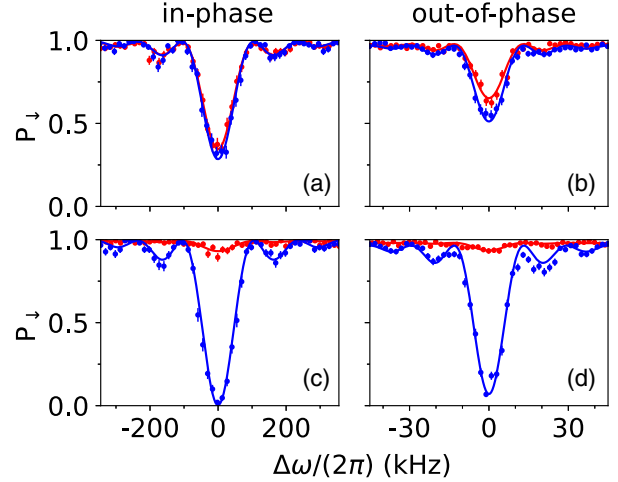


FIG. 4. Red and blue sidebands of the axial in- and out-of-phase modes of motion of $\text{H}_2^+ - {}^9\text{Be}^+$ probed using the stimulated Raman transition on ${}^9\text{Be}^+$. The detuning of the Raman lasers from the corresponding sideband transition is denoted $\Delta\omega$ and the measured ${}^9\text{Be}^+ |\downarrow\rangle$ probability P_{\downarrow} . The fits (solid lines) are used to extract the contrast and determine the average phonon number. We obtain for the in-phase mode (a) $\bar{n} = 10(5)$ after Doppler cooling and (c) $\bar{n} = 0.07(1)$ after sideband cooling. For the out-of-phase mode we obtain (b) $\bar{n} = 2.4(5)$ after Doppler cooling and (d) $\bar{n} = 0.05(1)$ after sideband cooling. For the dataset (c) the out-of-phase mode is Doppler cooled, while for the dataset (d) both the in- and out-of-phase mode are cooled to the ground state simultaneously. In the latter case, the temperature of the in-phase mode is similar to the one obtained from (c).

Doppler-cooled data for both the in- and out-of-phase mode is shown in Fig. 4. Since the data was taken at the π time of the corresponding sideband in the motional ground state, it demonstrates the achievable signal contrast for readout of the transfer mode in quantum logic protocols.

By performing the measurement of \bar{n} with different wait times after ground-state cooling, we derive a heating rate from the ground state of 9.3(4) quanta/s for the axial in-phase mode and 10.6(7) quanta/s for the axial out-of-phase mode. For the axial motion of a single ${}^9\text{Be}^+$ ion (mode frequency $2\pi \times 1.1$ MHz) we measure a heating rate of 4.2(3) quanta/s. These heating rates are low enough such that the axial in- and out-of-phase modes of $\text{H}_2^+ - {}^9\text{Be}^+$ can be used as transfer modes in quantum logic protocols, since they do not heat up considerably for an expected H_2^+ state readout duration [25].

We have reported on trapping and ground-state cooling of a $\text{H}_2^+ - {}^9\text{Be}^+$ ion pair, paving the way towards quantum control and high-precision spectroscopy of H_2^+ using QLS. Future implementation of QLS will require rovibrational state preparation of the H_2^+ . The electron-impact ionization that was used for this study creates the H_2^+ in a distribution of rovibrational states [45]. With He buffer-gas cooling, it should be possible to prepare the rovibrational ground state

of H_2^+ [20], and our apparatus has the capabilities necessary to test this approach. Another possibility may be to use REMPI to create H_2^+ in the desired rovibrational state [5,46]. Beyond H_2^+ , our apparatus and techniques are also suitable to control other light ion species, such as He^+ , H_3^+ , and HD^+ .

The authors thank B. MacDonald-de Neeve and C. Axline for technical support, the Segtrap and Penning teams of the ETHZ TIQI group for sharing laser light, and D. Leibfried, C.-W. Chou, D. R. Leibbrandt, D. B. Hume, Ch. Kurz, D. J. Wineland, D. T. C. Allcock, D. H. Slichter, S. Willitsch, L. Hilico, J.-Ph. Karr, F. Merkt, and M. Grau for helpful discussions and advice. This work was supported by Swiss National Science Foundation Grant No. 179909, by ETH Research Grant No. ETH-52 19-2, as a part of NCCR QSIT, a National Centre of Competence (or Excellence) in Research, funded by the Swiss National Science Foundation (Grants No. 51NF40-185902), and by EU Quantum Flagship H2020 FETFLAG-2018-03 under Grant Agreement No. 820495 AQTION.

*snick@phys.ethz.ch

†daniel.kienzler@phys.ethz.ch

- [1] J.-P. Karr, S. Patra, J. C. J. Koelemeij, J. Heinrich, N. Sillitoe, A. Douillet, and L. Hilico, *J. Phys. Conf. Ser.* **723**, 012048 (2016).
- [2] J.-P. Karr, L. Hilico, J. C. J. Koelemeij, and V. I. Korobov, *Phys. Rev. A* **94**, 050501(R) (2016).
- [3] H. O. Pilon, *J. Phys. B* **46**, 245101 (2013).
- [4] D. M. Bishop, S. Shih, C. L. Beckel, F. Wu, and J. M. Peek, *J. Chem. Phys.* **63**, 4836 (1975).
- [5] J. Schmidt, T. Louvradoux, J. Heinrich, N. Sillitoe, M. Simpson, J.-P. Karr, and L. Hilico, *Phys. Rev. Appl.* **14**, 024053 (2020).
- [6] L. Hilico (private communication).
- [7] S. Alighanbari, G. S. Giri, F. L. Constantin, V. I. Korobov, and S. Schiller, *Nature (London)* **581**, 152 (2020).
- [8] S. Patra, M. Germann, J.-P. Karr, M. Haidar, L. Hilico, V. I. Korobov, F. M. J. Cozijn, K. S. E. Eikema, W. Ubachs, and J. C. J. Koelemeij, *Science* **369**, 1238 (2020).
- [9] M. Beyer, N. Hölsch, J. A. Agner, J. Deiglmayr, H. Schmutz, and F. Merkt, *Phys. Rev. A* **97**, 012501 (2018).
- [10] N. Hölsch, I. Doran, M. Beyer, and F. Merkt, *J. Mol. Spectrosc.* **387**, 111648 (2022).
- [11] A. Osterwalder, A. Wüest, F. Merkt, and C. Jungen, *J. Chem. Phys.* **121**, 11810 (2004).
- [12] C. Haase, M. Beyer, C. Jungen, and F. Merkt, *J. Chem. Phys.* **142**, 064310 (2015).
- [13] E. G. Myers, A. Wagner, H. Kracke, and B. A. Wesson, *Phys. Rev. Lett.* **114**, 013003 (2015).
- [14] S. Hamzeloui, J. A. Smith, D. J. Fink, and E. G. Myers, *Phys. Rev. A* **96**, 060501(R) (2017).
- [15] S. Rau, F. Heiße, F. Köhler-Langes, S. Sasidharan, R. Haas, D. Renisch, C. E. Düllmann, W. Quint, S. Sturm, and K. Blaum, *Nature (London)* **585**, 43 (2020).
- [16] D. J. Fink and E. G. Myers, *Phys. Rev. Lett.* **124**, 013001 (2020).
- [17] D. J. Fink and E. G. Myers, *Phys. Rev. Lett.* **127**, 243001 (2021).
- [18] S. Schiller, D. Bakalov, and V. I. Korobov, *Phys. Rev. Lett.* **113**, 023004 (2014).
- [19] C. Wellers, M. R. Schenkel, G. S. Giri, K. R. Brown, and S. Schiller, *Mol. Phys.* **0**, e2001599 (2021).
- [20] S. Schiller, I. Kortunov, M. Hernández Vera, F. Gianturco, and H. da Silva, *Phys. Rev. A* **95**, 043411 (2017).
- [21] P. O. Schmidt, T. Rosenband, C. Langer, W. M. Itano, J. C. Bergquist, and D. J. Wineland, *Science* **309**, 749 (2005).
- [22] S. M. Brewer, J.-S. Chen, A. M. Hankin, E. R. Clements, C.-W. Chou, D. J. Wineland, D. B. Hume, and D. R. Leibbrandt, *Phys. Rev. Lett.* **123**, 033201 (2019).
- [23] P. Micke, T. Leopold, S. King, E. Benkler, L. Spieß, L. Schmoeger, M. Schwarz, J. Crespo López-Urrutia, and P. Schmidt, *Nature (London)* **578**, 60 (2020).
- [24] F. Wolf, Y. Wan, J. C. Heip, F. Gebert, C. Shi, and P. O. Schmidt, *Nature (London)* **530**, 457 (2016).
- [25] C.-W. Chou, C. Kurz, D. B. Hume, P. N. Plessow, D. R. Leibbrandt, and D. Leibfried, *Nature (London)* **545**, 203 (2017).
- [26] M. Sinhal, Z. Meir, K. Najafian, G. Hegi, and S. Willitsch, *Science* **367**, 1213 (2020).
- [27] C.-W. Chou, A. L. Collopy, C. Kurz, Y. Lin, M. E. Harding, P. N. Plessow, T. Fortier, S. Diddams, D. Leibfried, and D. R. Leibbrandt, *Science* **367**, 1458 (2020).
- [28] Y. Lin, D. R. Leibbrandt, D. Leibfried, and C.-W. Chou, *Nature (London)* **581**, 273 (2020).
- [29] J.-P. Karr, *J. Mol. Spectrosc.* **300**, 37 (2014).
- [30] D. Leibfried, *Appl. Phys. B* **123**, 10 (2016).
- [31] J.-S. Chen, S. M. Brewer, C.-W. Chou, D. J. Wineland, D. R. Leibbrandt, and D. B. Hume, *Phys. Rev. Lett.* **118**, 053002 (2017).
- [32] S. A. King, L. J. Spieß, P. Micke, A. Wilzewski, T. Leopold, J. R. Crespo López-Urrutia, and P. O. Schmidt, *Phys. Rev. X* **11**, 041049 (2021).
- [33] Y. Wan, F. Gebert, F. Wolf, and P. O. Schmidt, *Phys. Rev. A* **91**, 043425 (2015).
- [34] R. Rugango, J. E. Goeders, T. H. Dixon, J. M. Gray, N. B. Khanyile, G. Shu, R. J. Clark, and K. R. Brown, *New J. Phys.* **17**, 035009 (2015).
- [35] J. P. Home, in *Advances in Atomic, Molecular, and Optical Physics*, Advances In Atomic, Molecular, and Optical Physics Vol. 62, edited by E. Arimondo, P. R. Berman, and C. C. Lin (Academic Press, New York, 2013), pp. 231–277, 10.1016/B978-0-12-408090-4.00004-9.
- [36] D. J. Wineland, C. Monroe, W. M. Itano, D. Leibfried, B. E. King, and D. M. Meekhof, *J. Res. Natl. Inst. Stand. Technol.* **103**, 259 (1998).
- [37] See Supplemental Material at <http://link.aps.org/supplemental/10.1103/PhysRevLett.131.133003> for details on the apparatus, control of $H_2^+ - ^9Be^+$, and the loading procedure.
- [38] S. Ragg, C. Decaroli, T. Lutz, and J. P. Home, *Rev. Sci. Instrum.* **90**, 103203 (2019).
- [39] H.-Y. Lo, J. Alonso, D. Kienzler, B. C. Keitch, L. E. de Clercq, V. Negnevitsky, and J. P. Home, *Appl. Phys. B* **114**, 17 (2014).

- [40] M. Guggemos, D. Heinrich, O. Herrera-Sancho, R. Blatt, and C. Roos, *New J. Phys.* **17**, 103001 (2015).
- [41] Z. Meir, G. Hegi, K. Najafian, M. Sinhal, and S. Willitsch, *Faraday Discuss.* **217**, 561 (2019).
- [42] O. Asvany and S. Schlemmer, *Int. J. Mass Spectrom.* **279**, 147 (2009).
- [43] J. Glosík, *Int. J. Mass Spectrom. Ion Process.* **139**, 15 (1994).
- [44] F. Diedrich, J. C. Bergquist, W. M. Itano, and D. J. Wineland, *Phys. Rev. Lett.* **62**, 403 (1989).
- [45] Y. Weijun, R. Alheit, and G. Werth, *Z. Phys. D At. Mol. Clusters* **28**, 87 (1993).
- [46] Y. Zhang, Q.-Y. Zhang, W.-L. Bai, Z.-Y. Ao, W.-C. Peng, S.-G. He, and X. Tong, *Phys. Rev. A* **107**, 043101 (2023).